OCEANOGRAPHIC CHARACTERISATION OF THE CAPE VERDE REGION USING MULTISENSOR DATA

M. J. Fernandes[(1)], C. Lázaro[(1)], A. M. P. Santos[(2)], P. Oliveira[(2)]

(1) Faculdade de Ciências, Universidade do Porto
Departamento de Matemática Aplicada, 4169-007, Porto, Portugal
Tel: 00351 220 100 802, Fax: 00351 220 100 809
e-mail: mjfernan@fc.up.pt; clazaro@fc.up.pt

(2) Instituto Nacional de Investigação Agrária e das Pescas (INIAP) - IPIMAR
Departamento de Ambiente Aquático (DAA)
Av. Brasília, 1449-006 Lisboa, Portugal
Tel: 00351 213 027 193, Fax: 00351 213 015 948
e-mail: amsantos@ipimar.pt; pbo@ipimar.pt

ABSTRACT

This study focuses on the characterisation of the northeast Tropical Atlantic region ($3^oN \leq \varphi \leq 30^oN$, $40^oW \leq \lambda \leq 10^oW$) in terms of the main ocean circulation, sea surface temperature and associated phytopigment concentration patterns and their seasonal and interannual variability using multisensor remote sensing data.

The data include radar altimetry from ERS-2 and Topex/Poseidon used to derive absolute dynamic topography (ADT) and surface geostrophic currents, sea surface temperature (SST) from ATSR-2 and AVHRR and chlorophyll-a concentrations from SeaWiFS. The first two data sets (altimetry and SST from AVHRR) cover 8 years, from June 1995 to May 2003. The SST data set from ATSR-2 covers a period of 1 year, from June 2001 to May 2002. The chlorophyll-a data set comprises nearly 6 years, from September 1997 to May 2003.

The analysis of these data allowed the characterisation of the main current systems and their variability, the seasonal distribution of the SST and chlorophyll-a concentration and associated synergies between these data sets. The results of this analysis are discussed and the main conclusions are highlighted.

1. INTRODUCTION

In this study a time-series of remote sensing data is analysed in order to attempt the characterisation of the NE Tropical Atlantic surrounding the Cape Verde Archipelago. The study area is shown in Fig. 1.

Most of the present knowledge of the study area comes from several studies carried out in recent years supported by historical hydrographic data and more recently in situ observations [1], [2], [3], [4]. A seasonal signal of the NE tropical Atlantic large-scale surface circulation has been recognised as the oceanic response to the seasonal variability of the trade winds and the meridional displacement of the Intertropical Convergence Zone (ITCZ). This seasonal cycle is also present in the flow field along the NW African coast and in the associated upwelling. Although this seasonal signal is particularly strong in the southern part of the North Atlantic subtropical gyre large regions of the study area do not show a considerable seasonal cycle [2]. The total transport does not show, however, significant variations [5].

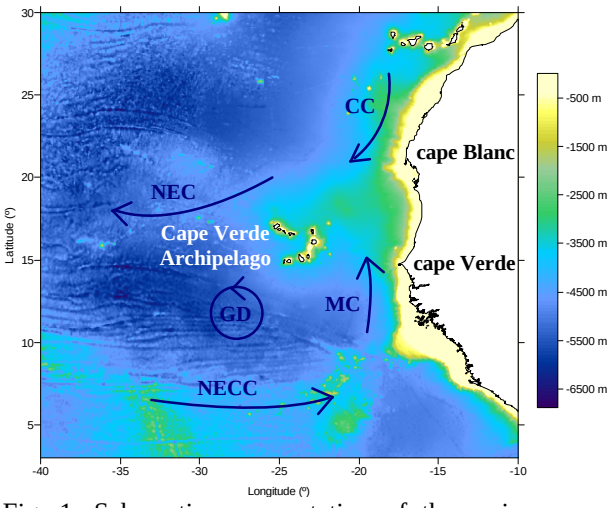

Fig. 1. Schematic representation of the major ocean circulation features presented in Cape Verde Archipelago region (acronyms explained in the text). Also shown is the location of capes Verde and Blanc.

The Cape Verde Archipelago is located at the eastern boundary of the North Atlantic subtropical gyre at the southern limit of the Canary Current (CC). The CC transports cool water southwards along the African coast and deviates from the coast between latitudes 25ºN and 20ºN, where it turns westwards and gradually becomes the North Equatorial Current (NEC) at lower latitudes [6].

Proc. of the 2004 Envisat & ERS Symposium, Salzburg, Austria
6-10 September 2004 (ESA SP-572, April 2005)

Between latitudes 5ºN and 10ºN, the dominant feature is the North Equatorial Countercurrent (NECC). The NECC shows a strong seasonal variation, being stronger in northern summer and autumn (from July through December) when the ITCZ reaches its northernmost position. During this period the NECC is a continuous zonal flow extending over almost the entire Tropical Atlantic [5], [6]. Some studies also suggest a related shift of the NEC to the north during this period due to the northward shift of the ITCZ [5]. During northern winter and spring the strong trade winds are responsible for the weakening of the NECC which at the same time also becomes irregular [6].

Therefore, the area between 10ºN and 15ºN, which includes the Cape Verde Archipelago, can be regarded as a region of large-scale interactions between the CC, the NEC and the NECC [6]. Different water masses meet in the vicinity of the archipelago forming a large-scale frontal system. The associated frontal zones are potentially productive zones, favourable for the aggregation of large pelagic highly migratory fish species.

As the NECC meets the African coast, some of its flow derives towards north resulting in a northward flow referred by some authors as the Mauritanian Current (MC), responsible for the carriage of warm oligotrophic equatorial water to the tropical eastern Atlantic.

The MC also shows a seasonal behaviour associated with the NECC. In winter and early spring the MC only reaches latitudes of about 14ºN (cape Verde). At this period of the year the wind field off the African coast south of 20ºN is favourable to the appearance of coastal upwelling. This cold and nutrient-rich upwelled water is transported southwards and is responsible for the high productivity of the region [6]. In summer and early autumn, due the strengthening of the NECC and the relaxation of NE trade winds, with its southern boundary in its northernmost limit (at about 21ºN off the coast), the MC reaches latitudes of about 20ºN, just south of cape Blanc (Fig. 1), and is responsible for the suppression of coastal upwelling south of 20º N [6].

Coastal upwelling is a permanent feature throughout the year between 20ºN and 25ºN with maximum intensity during spring and autumn [6], [4]. North and south of these latitudes, upwelling appears as a seasonal feature along the coast. South of 20ºN this phenomenon occurs during winter and spring. North of 25ºN the upwelling season generally occurs in summer and early autumn.

Another interesting feature in the study region is the Guinea Dome (GD) a constituent of the large-scale near-surface flow fields associated with the NEC, the NECC and the North Equatorial Undercurrent (NEU) [1]. The GD is located southwest of Cape Verde Archipelago and has an associated cyclonic geostrophic flow. It exists permanently throughout the year at NEU levels while seasonal variations are found above [1]. It is suggested that the associated flow weakens in winter, probably caused by the similar seasonal change in the NECC [1].

2. DATA USED AND PROCESSING

In this study three main types of satellite data have been used: absolute dynamic topography (ADT) and derived surface geostrophic currents from the Radar Altimeters (RA) onboard ERS-2 and Topex/Poseidon (T/P), sea surface temperature (SST) from ATSR-2 (Along-Track Scanning Radiometer) and AVHRR (Advanced Very High Resolution Radiometer) and chlorophyll-a concentrations from SeaWiFS (Sea-viewing Wide Field-of-view Sensor).

The RA and SST (AVHRR) data cover a period of 8 years, from June 1995 to May 2003. The SST data set from ATSR-2 covers a period of 1 year, from June 2001 to May 2002. The chlorophyll-a data set comprises nearly 6 years, from September 1997 to May 2003.

Tuna catch and effort data were provided by the International Commission for the Conservation of Atlantic Tunas (ICCAT) for the period 1995-1997, and were analysed in conjunction with the satellite data.

2.1 Altimeter Data

The analysed altimeter data include ERS-2 and T/P. The ERS-2 data are the OPR02 precise geophysical products provided by ESA [7], from cycles 1 to 85. The spatial resolution of these data in the study region varies from 80 km at latitude 3ºN to about 69 km at latitude 30ºN. The temporal resolution is 35 days. The T/P data are the GDR-M products provided by AVISO [8], with a spatial resolution of 315 km at latitude 3ºN and approximately 273 km at latitude 30ºN and a temporal resolution of 10 days.

From the geophysical products, corrected sea surface heights (SSH) were derived by applying to data all relevant geophysical corrections, as described in [9] and [10]. Sea Level Anomalies (SLA) were derived by subtracting the Mean Sea Surface (MSS) height from the GSFC2000 model [11] to the corrected SSH values.

For the analysed period of eight years (June 1995 to May 2003) monthly maps of ADT and geostrophic currents were derived using the procedure described below:

- ERS-2 35-day and T/P 10-day data were split into monthly files (containing data centred on each month

of the year, including 35 days of ERS-2 and 365.25/12 days of T/P data). This procedure was adopted to get full ERS-2 coverage.

- Each ERS-2 file was crossover adjusted to the corresponding T/P data file, using tilt and bias parameters. The ERS-2 (adjusted) and T/P data were joined together, creating monthly files of merged data.
- Monthly grids of Sea Level Anomalies (SLA) were computed using the kriging method implemented in the commercial software SURFER. A data spacing of 3 arc minutes has been used. To reduce the effect of trackiness and enhance data visualisation, the SLA grids were filtered using a low pass Butterworth filter of second order with a cut-off half-wavelength of 150 km.
- Monthly ADT grids were generated by adding to each SLA grid the mean dynamic topography modelled by the global ocean circulation model Parallel Ocean Climate Model 4B (POCM_4B) [12].
- From the ADT grids, sea surface currents along the zonal and meridional directions were computed, using the known geostrophic equations [13].

The method adopted to derive the ADT is one of the possible methods that can be used while a sufficiently accurate global geoid model is not available [14]. The mean dynamic topography used here was modelled by a twenty year mean run from the ocean circulation model POCM_4B, also known as Semtner & Chervin model.

2.2 SST Data

- **AVHRR Data**

Eight years of SST distributions were obtained from the NOAA/NASA AVHRR Oceans Pathfinder v.4.1. These are monthly SST values derived from the AVHRR radiometers on board the NOAA -7, -9, -11 and -14 polar orbiting satellites. The products used are given on equal-angle grids of 4096×2048 pixels (referred to as the ~9 km grid), and data used were only from the ascending pass (daytime).

- **ATSR Data**

ATSR-2 Gridded Sea Surface Temperature (GSST) products available from ATSR Near Real Time Service (NRTS) were processed for ERS-2 cycles 64 (May 2001) to 73 (May 2002). These gridded products (512×512 pixels) have a spatial resolution of 1 km×1 km. Only GSST products from ERS-2 descending passes were available for the NE Atlantic, which leads to a maximum of 90 products covering the study area for each cycle.

The GSST products were processed into image form, cloud-masked, land-masked and geo-located. SST values were truncated to 0.1ºC and temperatures outside the range 10ºC–30ºC were considered noise. Nadir View SST images for each ERS-2 cycle were used to create synoptic maps representing averaged SST values.

2.3 SeaWiFS Data

The ocean colour data were obtained from the NASA Distributed Active Archive Center at the Goddard Space Flight Center. The product used was the Level-3 standard mapped images (SMI) of monthly chlorophyll-a (Chl-a) concentrations from the SeaWiFS on board the OrbView-2 polar orbiting satellite, which is given in a 9 km grid. The Chl-a concentration was computed using the bio-optical algorithm OC4v4 (*e.g.* [15]).

2.4 Fisheries Data

Tuna catch per unit of effort (cpue), in metric tons per fishing hour, were computed based on monthly catch and effort data (1995-1997) provided by the ICCAT with a spatial aggregation of 1ºx1º latitude-longitude rectangle. Tuna catch corresponds to the sum of the catches for yellowfin (*Thunnus albacare*), bigeye (*T. obesus*) and skipjack (*Katsuwonus pelamis*) tuna. Two types of fisheries (fishing gear) were analysed separately: the purse-seine fishery, more industrial and oceanic; and the more artisanal and coastal bait-boat fishery. We defined "very good" catches for cpue > 3.5 tons/fishing hour which correspond to a percentile of 90 for the purse-seine fishery and of 95 for the bait-boat fishery.

3. RESULTS

Geostrophic surface currents were computed for each ADT grid and represented as vectors overlaid in ADT coloured maps. Due to the differences in geostrophic velocities between the northernmost and southernmost regions of the study area, the geostrophic velocities were scaled by a linear function of latitude. In this way, the geostrophic velocities for latitude 30º N are represented by arrows 4 times greater than they would be if the velocity scale was maintained in the meridional direction. This procedure allows a better analysis of the ocean circulation patterns in the northernmost region of the study area.

From this analysis, a strong seasonal signal is clearly visible, particularly in the southernmost region of the study area. During May and June, the NECC is visible as the zonal flow east of 25º W and centred in latitudes 5ºN. In July, this flow strengthens, becomes a clearly continuous zonal flow and occupies all the study area, between latitudes 5º N and 8º N. During August and September the NECC is in its northernmost position and is strongest during this period. This condition is

depicted in Fig. 2. From October, the NECC becomes irregular and this situation increases until December, when only large anticyclones are seen in these latitudes. During the first two months of the year there is no signal of a zonal flow in the study region (Fig. 3). During March and April, the NECC starts to develop and is only seen eastern of longitudes 20º W. During the period from December to June, the southward current along the African coast strengths. From the ADT maps the CC is stronger during the months from April to June. Its weakening is verified after July and the CC seems to be weaker in November.

The GD is clearly seen in ADT maps during summer and autumn. It is, in general, located southwest of Cape Verde Archipelago and exhibits a strong cyclonic geostrophic flow during the period from July to October (Fig. 2). Seasonal variations are found since the GD weakens from December, probably due the similar seasonal change in the NECC, being minimum in February/March. During May a cyclonic feature is seen southeast of the Cape Verde Archipelago that seems to propagate westwards during June and July.

The seasonal signal along the NW Africa coast is strongly linked with coastal upwelling variability forced by the north-south migration of trade winds present in the region. From December to May the band of cold and pigment-rich upwelled waters extends as far south as 10º N. This can be seen in Fig. 4 and 5 which represent monthly mean values for the whole corresponding data sets. This is associated with the strengthening of the Canary Current and the weakening of the NECC during this period (Fig. 3 and 5).

From June to November, the upwelling relaxation is accompanied by the northward extension of the NECC transporting warm oligotrophic waters, which reach the latitude of 20º N around August (Fig. 2, 4 and 5).

The change in the SST distribution follows the ICTZ meridional seasonal migration. In the offshore region, the seasonal amplitude of SST is much lower than in the coastal region and achieves maximum values from September to November, when higher pigment concentrations are observed in the vicinity of Cape Verde islands (Fig. 7).

The averaged SST monthly maps obtained from ATSR-2 data show bad coverage of the study area compared with the AVHRR maps. This is due to the use of GSST products from ERS-2 descending passes only (leading to few products covering the study area for each cycle), to the continuous cloud contamination of the study area and to lower temporal resolution of the ATST-2 sensor. Nevertheless the results described above are also depicted in the analysed ATSR-2 data.

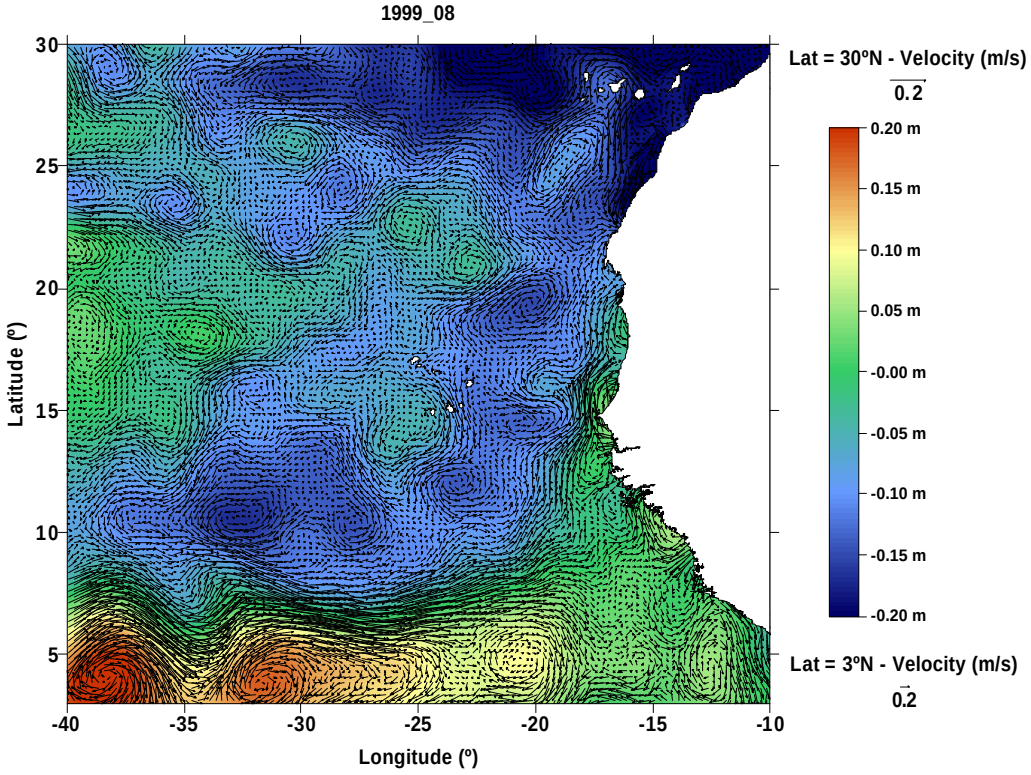

Fig. 2. ADT and geostrophic surface currents for August 1999 (note that the geostrophic velocities were scaled by a linear function of latitude).

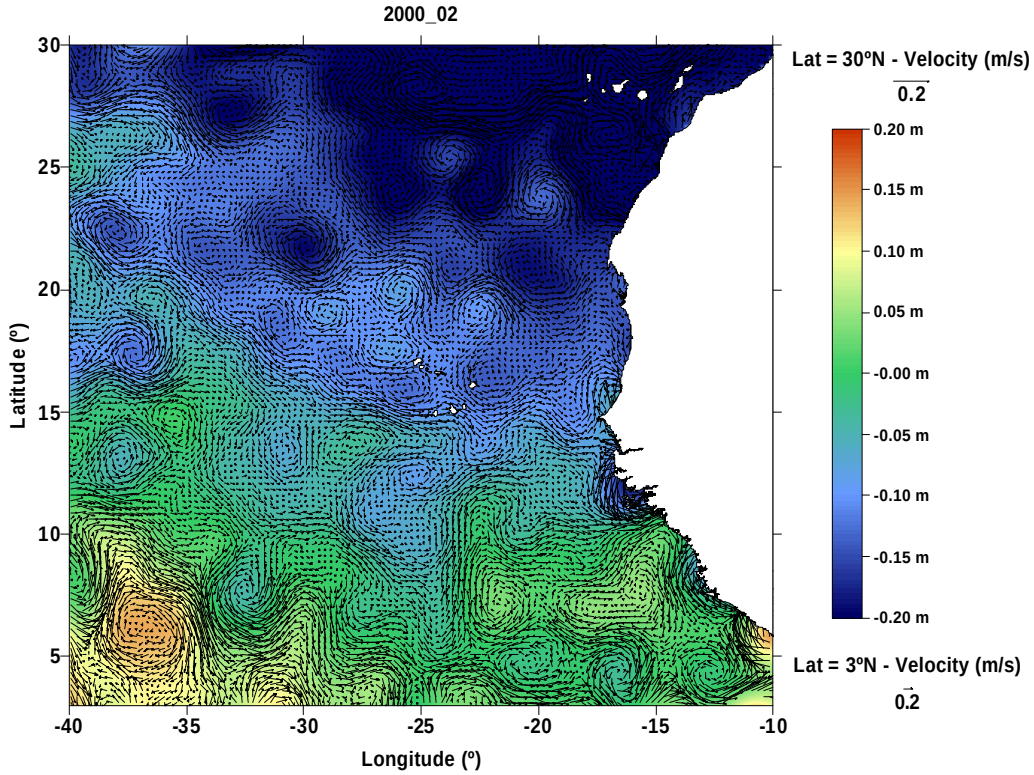

Fig. 3. ADT and geostrophic surface currents for February 2000 (note that the geostrophic velocities were scaled by a linear function of latitude).

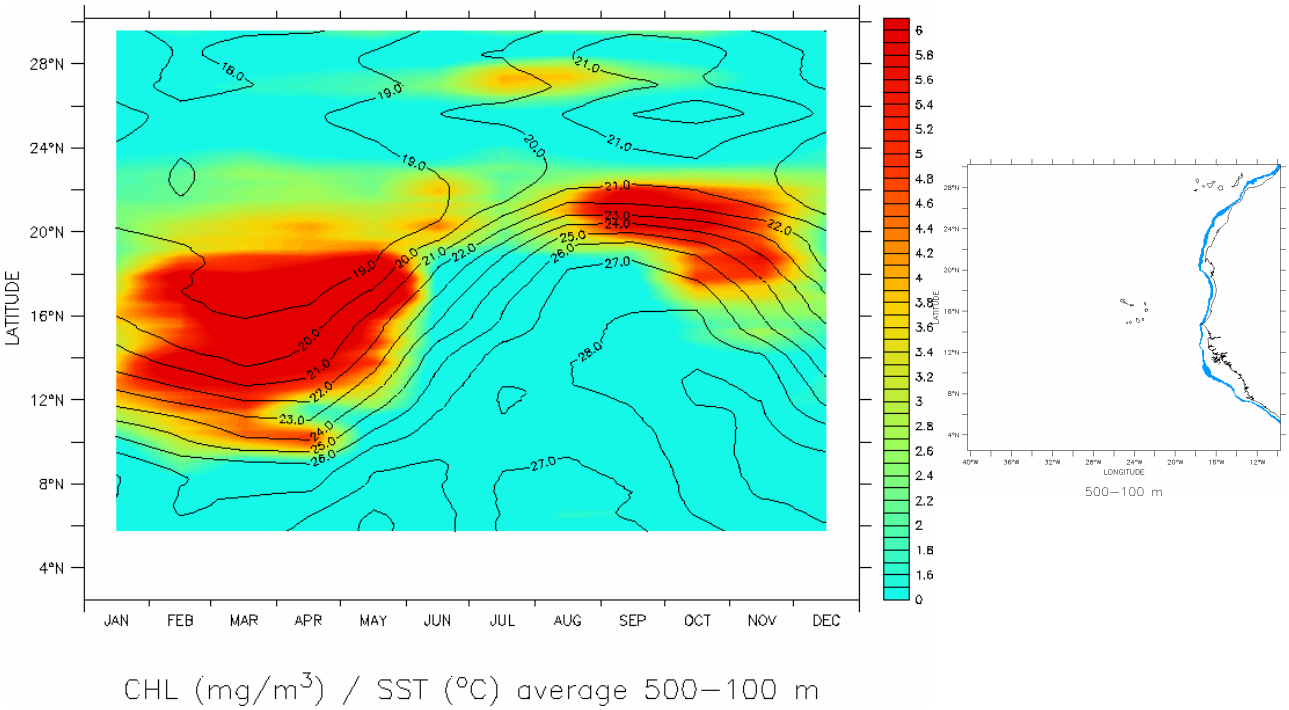

Fig. 4. Seasonal cycle of SST (black lines) and Chl-a (colour shade) along the coast of NW Africa. The monthly mean values were computed for the 8 years period of SST and 6 years of Chl-a data obtained along the blue line on the right panel.

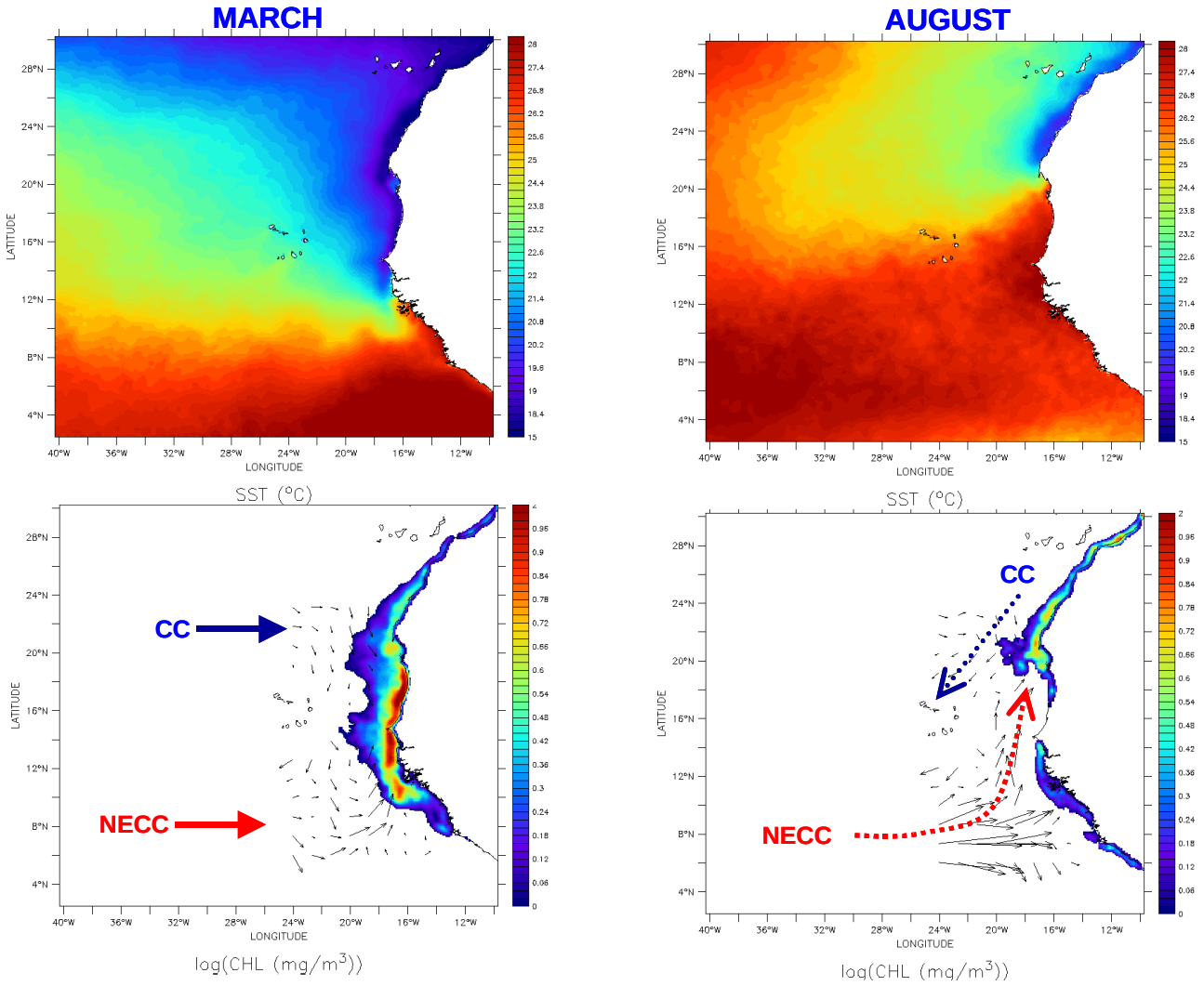

Fig. 5. Monthly mean distributions for March and August, for the whole study period, of SST (top) and Chl-a concentrations (bottom) off the NW Africa. The black arrows on the Chl-a images are geostrophic currents computed from ADT data. The Canary Current (CC) and the North Equatorial Countercurrent (NECC) are indicated.

Several cyclonic/anticyclonic structures visible in the current fields can be associated with regions of high/low chlorophyll-a concentration.

A large interannual variability is observed in all the fields, being particularly evident in the distributions of chlorophyll-a.

Examples of this are: (i) in March 1999, the coastal upwelling was very intense and extended along almost all the coastal region; (ii) during October 1997 extensive phytoplankton blooms (~2 x 10^5 km^2), characterised by chlorophyll-a concentrations ~40 times greater than the adjacent waters, were observed in offshore oligotrophic waters (~1200 km from the coast) (Fig. 6). During this year the GD was particularly strong during the former months (August and September).

Another interesting feature is the extension of the giant filament of Cape Blanc, which during certain years (e.g., 1999 and 2001) could act as a source of pigment-rich waters for the Cape Verde islands waters (Fig. 7). The pigment-rich waters observed in Fig. 7 had a displacement of about 430 km between September-October 1999 and 230 km between October-November 1999, corresponding to an advection speed of 0.16 m/s and 0.09 m/s, respectively. These values are compatible with the geostrophic currents estimated from ADT.

The results were compared with tuna catch per unit of effort (cpue) data, although their low spatial and temporal resolution makes this type of analysis difficult.

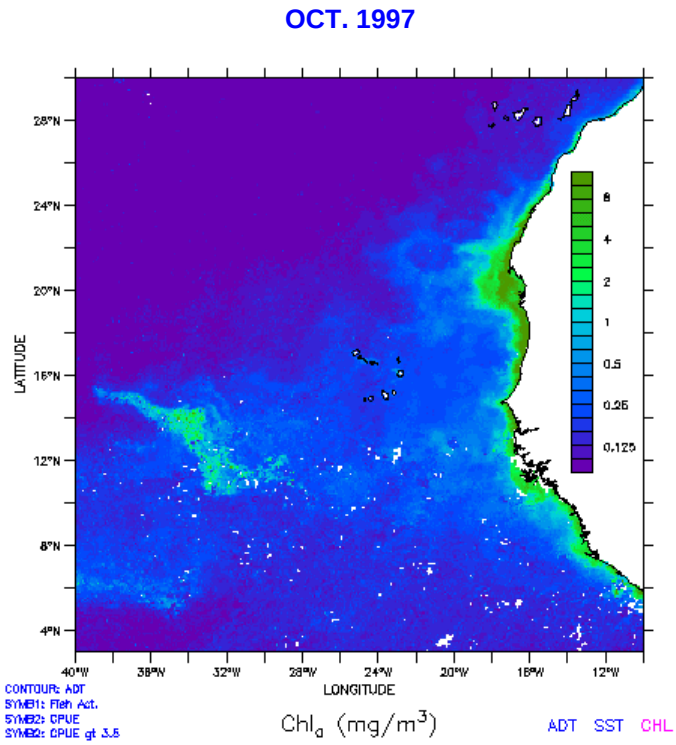

Fig. 6. SeaWiFS-derived monthly mean chlorophyll-a concentration during October 1997 off NW Africa, showing a massive phytoplankton bloom in offshore oligotrophic waters.

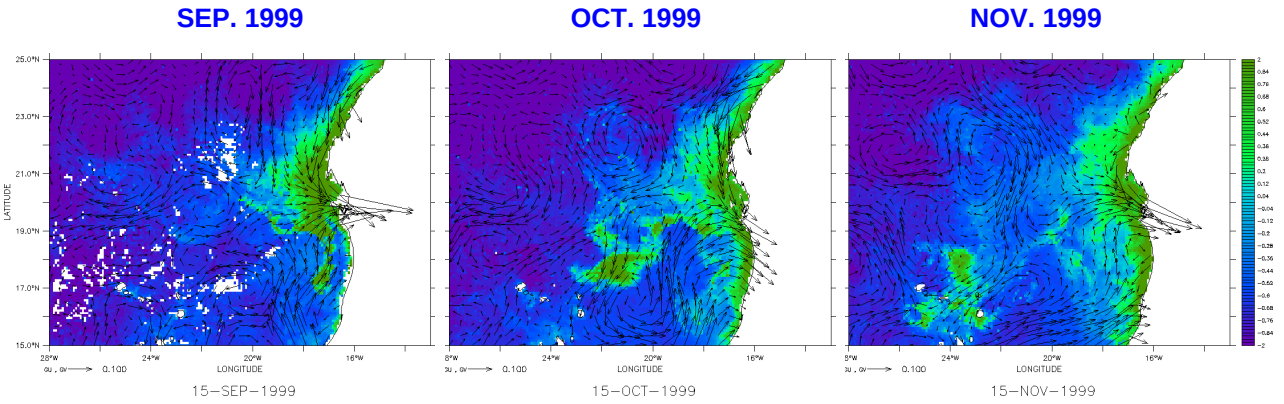

Fig. 7. SeaWiFS-derived monthly mean chlorophyll-a concentrations during September-November 1999 off NW Africa. The arrows are the estimated geostrophic currents from ADT. This figure shows the offshore advection of the giant filament of Cape Blanc.

The activity of the purse-seine fishery during 1995-1997 was usually associated with a cyclonic circulation off the Guinea-Senegal coast (the Guinea Dome), clearly seen in the ADT maps (Fig. 8). The enhanced productivity in the surface waters above these domes, coupled with the shallowing of the thermocline could explain the success of the fishing activity associated with this feature.

The bait-boat fishery operates mainly in the Cape Verde-Mauritania region, linked with the upwelling season. It is interesting to note that in this case the success of the fishery seems to be associated with the warm waters adjacent to the cold pigment-rich upwelled waters (Fig. 9). However, the limitation of the fishing data (low spatial resolution and small period of time) does not allow conclusive results.

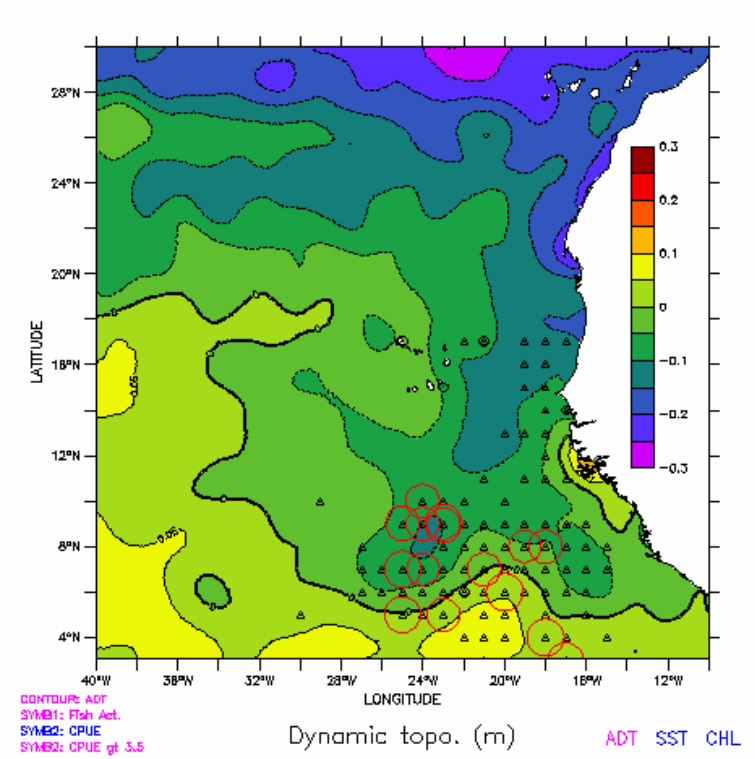

Fig. 8. Purse-seine tuna fishing activity (triangles) off NW Africa during May 1997 superimposed on the absolute dynamic topography (ADT) for the same month. The red circles represent “very good” catches (cpue > 3.5 tons/fishing hour). The Guinea Dome is located between about 6º-10º N and 26º-20º W.

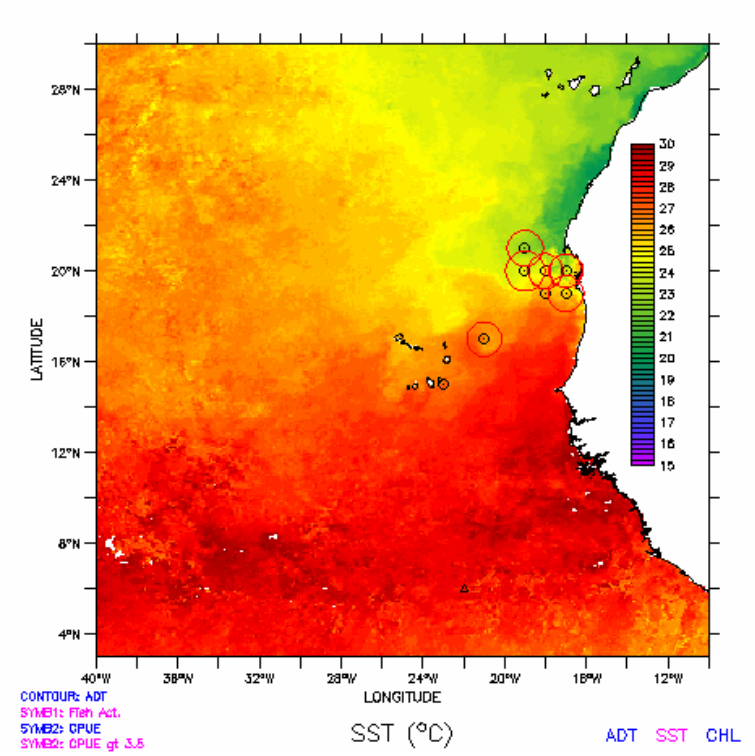

Fig. 9. Bait-boat tuna fishing activity (small black circles) off NW Africa during October 1996 superimposed on the sea surface temperature (SST) for the same month. The red circles represent “very good” catches (cpue > 3.5 tons/fishing hour).

4. CONCLUSIONS

The method adopted to derive the ADT is one of the possible methods that can be used while a sufficiently accurate global geoid model is not available. In spite of this restriction, the main ocean circulation patterns and their seasonal and interannual variability are clearly depicted in the derived ADT maps.

A local gravimetric geoid has been computed [16] using the available marine gravity provided by the Bureau Gravimetrique International (BGI). These data have a very uneven spatial distribution and variable accuracy, usually not better than a few mGal. The ADT derived by using this geoid model was found to be inadequate for the purpose of this study, particularly in the centre of the study region, around the Cape Verde archipelago.

The derived ADT showed strong gradients around the islands, partly due to the absence of land gravity in the geoid solution and partly due to the lower accuracy in the altimeter data close to land.

Only after 2006, as a result of the ESA gravity mission GOCE, a centrimetric global geoid is expected with a resolution (half wavelength) of about 55 km, adequate for mesoscale studies.

Using a synergetic analysis of satellite-derived information it was possible to describe the seasonal and interannual variability of the ocean circulation and several relevant features (e.g., Guinea dome, coastal upwelling) off NW Africa. The ADT information was very useful, for example in the detection of the Guinea dome since the upward movement of the thermocline does not reach the surface and thus it is difficult to be detected in the SST distributions. Using ocean colour information, complemented with geostrophic currents derived from ADT data, it was possible to follow the evolution of upwelling coastal filaments and its propagation to the open ocean.

Although fisheries data had low resolution, it was possible to link the fishing activity with features like coastal upwelling filament fronts and the Guinea dome. This association of tuna with the warm side of upwelling fronts and thermal domes are in accordance with previous studies (e.g., [17]; [18] and [19]).

5. AKNOWLEDGMENTS

This study has been funded by FCT project POCTI/36095/CTA/2000. The ERS-2 altimeter and ATSR data have been provided by ESA under the scope of the project “Remote Sensing Applied to Fisheries in the Cabo Verde Region”, AO3-265. The remote sensing activities of INIAP-IPIMAR are partially conducted under the SIGAP Project (22-05-01-FDR-00013). For the use of the satellite and fisheries data acknowledgements are due to the SeaWiFS Project (Code 970.2) and the Distributed Active Archive Center (Code 902) at the Goddard Space Flight Center for the production and distribution of ocean colour data, to the NASA PO-DAAC at the Jet Propulsion Laboratory for the SST Pathfinder data, and to ICCAT for making available tuna catch and effort data. Finally, we want to acknowledge the use of Ferret freeware software that is a product of NOAA- Pacific Marine Environmental Laboratory.

6. REFERENCES

1. Siedler, G., N. Zangenberg, R. Onken, A. Molière, Seasonal Changes in the Tropical Atlantic Circulation: Observation and Simulation of the Guinea Dome, *Journal of Geophysical Research*, Vol. 97, C1, 703–715, 1992.

2. Stramma, L. and F. Schott, The mean flow field of the tropical Atlantic Ocean, *Deep-Sea Research II*, 46 279–303, 1999.

3. Stramma, L. and H. Isemer, Seasonal variability of meridional temperature fluxes in the eastern North Atlantic Ocean, *Journal of Marine Research*, 46, 281–299, 1988.

4. Ould-Dedah, S., W. J. Wiseman Jr., R. F. Shaw, Spatial and temporal trends of sea surface temperature in the northwest African region, *Oceanologica Acta*, 22, Nº. 3, 265–279, 1999.

5. Stramma, L. and G. Siedler, Seasonal Changes in the North Atlantic Subtropical Gyre, *Journal of Geophysical Research*, Vol. 93, Nº. C7, 8111–8118, 1988.

6. Mittelstaedt, E., The ocean boundary along the northwest African coast: Circulation and oceanographic properties at the sea surface, *Progress in Oceanography*, Vol. 26, 307–355, 1991.

7. ESA (European Space Agency), *Altimeter & Microwave Radiometer ERS Products User Manual*, C2-MUT-A-01-IF, 1996.

8. AVISO/Altimetry, *AVISO User Handbook for Merged TOPEX/POSEIDON products*, AVI-NT-02-101_CN, Edition 3.0, 1996.

9. Fernandes, M. J. and M. Antunes, Eight Years of Satellite Radar Altimetry in The Northeast Atlantic, *Proceedings of the 3ª Assembleia Luso-Espanhola de*

Geodesia e Geofísica, Vol I, 226–230, Garcia F. and Valero, J. (Ed.), Editorial UPV, 2002.

10. Fernandes, M. J., L. Bastos and M. Antunes, Coastal Satellite Altimetry – Methods for Data Recovery and Validation, *Proceedings of the 3rd Meeting of the International Gravity & Geoid Commission* (GG2002), 302–307, Tziavos, I. N. (Ed.), Editions ZITI, 2002.

11. Wang, Y. M. *GSFC00* Mean Sea Surface, Gravity Anomaly, and Vertical Gravity Gradient from Satellite Altimeter Data, *Journal of Geophysical Research*, 106, 31167– 31174, 2001.

12. Stammer, D., R. Tokmakian, A. Semtner and C. Wunsch, How Well Does a ¼º Global Circulation Model Simulate Large-Scale Oceanic Observations?, *Journal of Geophysical Research*, 101, 25779–25811, 1996.

13. Knudsen, P., Integration of gravity and altimeter data by optimal estimation techniques, In *Satellite Altimetry in Geodesy and Oceanography*, Rummel and Sanso (Ed.), Springer Verlag, 453–466, 1993.

14. Le Traon, P.Y. and R. Morrow, Ocean currents and mesoscale eddies, In *Satellite Altimetry and Earth Sciences*, Fu, L. and A. Cazenave (Ed.), Academic Press, 2001.

15. O'Reilly, J.E., Maritorena, S., Siegel, D.A., O'Brien, M.C., Toole, D., Mitchell, B.G., Kahru, M., Chavez, F.P., Strutton, P., Cota, G.F., Hooker, S.B., McClain, C.R., Carder, K.L., Müller-Karger, F., Harding, L., Magnuson, A., Phinney, D., Moore, G.F., Aiken, J., Arrigo, K.R., Letelier, R., Culver, M., Ocean color chlorophyll-a algorithms for SeaWiFS, OC2, and OC4: Version 4, In *SeaWiFS postlaunch calibration and validation analyses, Part 3*, Hooker, S.B. and Firestone, E. R. (Ed.), NASA Technical Memorandum 2000-206892, Vol. 11, NASA Goddard Space Flight Center. Greenbelt, Maryland, pp. 9-23, 2000.

16. Fernandes, M. J., A. R. S. Marçal, J. C. Azevedo, A. M. P. Santos, A. Peliz, Fisheries Monitoring in The Cabo Verde Region Using ERS Data, *Proceedings of the ERS - ENVISAT Symposium, Looking down to Earth in the New Millenium*, Gothenburg, Sweeden, 16–20 October, 2000, ESA SP–461, paper Nº. 363, 2000.

17. Laurs, R. M., P. C. Fiedler and D. R. Montgomery, Albacore tuna catch distributions relative to environmental features observed from satellites. *Deep-Sea Research I*, 31(9), 1085-1099, 1984

18. Fonteneau, A. and J. Marcille (Ed), Resources, fishing and biology of the tropical tunas of the Eastern Central Atlantic. *FAO Fisheries Document Paper No. 292*, Rome, FAO. 354 p., 1993.

19. De Anda-Montanez, J. A., S. Martinez-Aguilar, A. Amador-Buenrostro and A. Muhlia-Almazán, Spatial Analysis of the Yellowfin Tuna (Thunnus albacares) Fishery, and its Relation to El Niño and La Niña Events in the Tropical Eastern Pacific. *Investig. mar.*, 30 (1 supl), 178-179, 2002.